Taylor, L. L., Quirk, J., Thorley, R. M. S., Kharecha, P. A., Hansen, J., Ridgwell, A., Lomas, M. R., Banwart, S. A., & Beerling, D. J. (2016). Enhanced weathering strategies for stabilizing climate and averting ocean acidification. *Nature Climate Change*, *6*(4), 402-406. https://doi.org/10.1038/nclimate2882

Enhanced weathering strategies for stabilizing climate and averting ocean acidification

Lyla L. Taylor[1], Joe Quirk[1], Rachel M.S. Thorley[1], Pushker A. Kharecha[2,3], James Hansen[2], Andy Ridgwell[4,5], Mark R. Lomas[6], Steve A. Banwart[7] & David J. Beerling[1*]

[1]Department of Animal and Plant Sciences, University of Sheffield, Sheffield S10 2TN, UK
[2]Earth Institute, Columbia University, 475 Riverside Drive, New York, 10027, USA
[3]Goddard Institute for Space Studies, NASA, 2880 Broadway, New York, 10025, USA
[4]Department of Geographical Sciences, University of Bristol, Bristol BS8 1SS, UK
[5]Department of Earth Sciences, University of California, Riverside CA, 92521, USA
[6]Department of Mathematics, University of Sheffield, Sheffield S10 2TN, UK
[7]Kroto Research Institute, North Campus, University of Sheffield, Sheffield S3 7HQ, UK

*Email d.j.beerling@sheffield.ac.uk

Chemical breakdown of rocks, 'weathering', is an important but very slow part of the carbon cycle that ultimately leads to CO_2 being locked-up in carbonates on the ocean floor. Artificial acceleration of this carbon sink via distribution of pulverized silicate rocks across terrestrial landscapes may help offset anthropogenic CO_2 emissions[1-5]. We show that idealized enhanced weathering scenarios over less than a third of tropical land could significantly drawdown atmospheric CO_2 and ameliorate ocean acidification by 2100. Global carbon cycle modelling[6-8] driven by ensemble Representative Concentration Pathway (RCP) projections of 21st century climate change (RCP8.5, business-as-usual; RCP4.5, medium-level mitigation)[9,10], indicates that enhanced weathering could lower atmospheric CO_2 by 30-300 ppm by 2100 depending mainly on silicate rock application rate (1 kg or 5 kg m^{-2} yr^{-1}) and composition. At the higher application rate, end-of-century ocean acidification is reversed under RCP4.5 and reduced by about two-thirds under RCP8.5. Additionally, surface ocean aragonite saturation state, a key control on coral calcification rates, is maintained above 3.5 throughout the low latitudes, thereby helping maintain the viability of tropical coral reef ecosystems[11-14]. However, we highlight major issues of cost, social acceptability, and potential unanticipated consequences that will limit utilization and emphasize the need for urgent efforts to phase down fossil fuel emissions[15].

In 1992, over 170 nations agreed to limit anthropogenic CO_2 emissions to avoid 'dangerous' human-made climate change[16], yet massive expansion of fossil fuel extractions, including shale gas and tar sands, is allowing emissions to grow[17]. Avoiding dangerous climate change may therefore require the controversial deployment of Carbon Dioxide Removal (CDR) schemes[4,18], so called 'negative emissions' strategies whereby CO_2 is captured and removed from the atmosphere. The Fifth Assessment Report of the Intergovernmental Panel on Climate Change[12] and the U.S. National Research Council Report[18] both recognized enhanced terrestrial weathering of silicate rocks as an important but poorly constrained CDR approach. Currently, natural weathering of silicate and carbonate rocks consumes ~0.25 Pg C yr^{-1} of atmospheric CO_2, which is ~3% of fossil fuel emissions[19] (~9–10 Pg C yr^{-1}). Artificially accelerating this land-based CO_2 sink involves the intentional application of pulverised silicate rocks to vegetated landscapes to markedly enhance CO_2 consumption[1-5]. However, assessments to date have excluded primary drivers of soil mineral weathering, especially terrestrial ecosystem processes and feedbacks from CO_2 and future climate change, limiting our understanding of its capacity to offset fossil fuel CO_2 emissions[12].

Here we present spatially resolved analyses of enhanced weathering by terrestrial ecosystems as a macro-engineering CDR option based on idealized cases for distributing pulverised silicate rocks in the tropics using multi-model ensemble projections (Coupled Model Intercomparison Project, CMIP5) of 21st century climate change[9,10]. Our modelling framework includes climate-plant-soil linkages important for regulating mineral weathering by coupling a detailed weathering model with a dynamic global vegetation model and accounting for land surface hydrology, topography and lithology[6,7] (Methods). We assess effects of enhanced weathering on net CO_2 consumption and examine feedbacks on atmospheric CO_2 and ocean chemistry over the next century using a suite of five CMIP5 general circulation model (GCM) simulations (1°lat. × 1°lon.)[9,10] for each of two Representative Concentration Pathway scenarios (RCPs): RCP8.5 (business-as-usual), and RCP4.5 (medium-level stabilization of emissions); postscripts (8.5 and 4.5) denote radiative forcing (W m^{-2}) in year 2100 relative to year 1750 (Supplementary Information). Assessments are undertaken for various application rates of the igneous rocks dunite (>90% olivine, Mg_2SiO_4) (Ref. 3) and harzburgite (50–90% olivine), which are both commercially mined, and basalt for which major resources exist in terrestrial large igneous provinces (LIPs)[20] (Fig. 1). These rates fall within the range adopted in the early 1930s for rejuvenating European forest soils with basalt to encourage tree growth[21].

Our simulations indicate that terrestrial weathering can be markedly increased by distributing pulverised silicate rocks throughout the tropics (30°N to 30°S), potentially consuming hundreds of petagrams (1×10^{15} g) of CO_2 by 2100 (Fig. 1). Ensemble median CO_2 consumption by terrestrial weathering increases towards a maximum as the total rock applied increases, with olivine-rich dunite and harzburgite being about twice as effective as basalt for equivalent application rates (Fig. 1a–c). We present CO_2 consumption curves assuming mixing depths of 10 cm and 30 cm for each application rate; 10 cm is likely the minimum mixing depth given intense precipitation events, the distribution of macropores and bioturbation by invertebrates in tropical soils down to depths of 30–50 cm (Supplementary Information). In the model, CO_2 consumption by weathering increases when added rock grains mix deeper in the soil, particularly at the 5 kg m^{-2} yr^{-1} application rate, because mineral saturation, a chemical brake on weathering, occurs more slowly in a larger soil solution volume. Overall CO_2 consumption patterns for a particular RCP scenario show a consistently narrow range of variation across the five ensemble GCMs (Fig. 1d–f). For a given application rate, the magnitude of CO_2 consumption is similar for the business-as-usual (RCP8.5) and medium level mitigation (RCP4.5) scenarios (Fig.1d–f), largely because the runoff for the two scenarios is similar (Supplementary Information).

Comparing cumulative end-of-century amounts of pulverised rock added to the tropics with estimated total resources indicates dunite has limited utility for long-term atmospheric CO_2 removal[3] (Fig. 1), whereas sufficient harzburgite and basalt resources exist for the application rates considered here (Fig. 1, Supplementary Information). The rock mass required can be reduced by restricting application to regional intense tropical weathering 'hotspots' (Fig. 1, Supplementary Information). Such optimization reduces the land area required by more than two-thirds, from 69 Mkm^2 to 20 Mkm^2, and total rock mass by 70%, whilst still achieving ~80–89% of the effect (Fig. 1a–c, symbols). Hotspot land areas are primarily tropical forests except parts of Asia which are croplands. However, basalt can promote crop growth on highly weathered acidic tropical soils[22,23] by increasing soil alkalinity, cation exchange capacity and the availability of growth-limiting phosphorus, with associated reductions in Al and Mn toxicity[23,24]. Ample basalt resources exist within the major LIPs in the tropics (Ethiopian Traps, Deccan Traps and Paraná Traps) to support simulated application rates (Fig. 1) and these sources could exploit existing infrastructure for distribution. Meeting silicate rock demand would require large-scale mining operations, e.g.,

98 throughout the major tropical LIPs, with production rates exceeding those for coal and
99 adverse consequences for local ecosystems.

100 As CO_2 is removed from the atmosphere by enhancement of the weathering carbon sink,
101 the carbon cycle responds by redistributing carbon among surface reservoirs (atmosphere,
102 ocean, soil, and land biosphere), with CO_2 out-gassing by the ocean in particular offsetting
103 some of the artificial drawdown[17]. There is, consequently, a 'rebound' effect whereby each
104 extra mole of CO_2 consumed does not translate into the removal of a mole of atmospheric
105 CO_2 over time. We therefore estimate the effects of our CO_2 consumption fluxes on the
106 RCP4.5 and RCP8.5 atmospheric CO_2 trajectories through the 21st century with the well-
107 tested GENIE Earth system model[8] that broadly captures these responses. Distributing 1kg m^{-2}
108 yr^{-1} of pulverised silicates across 20 Mkm^2 of tropical weathering 'hotspots' lowers
109 atmospheric CO_2 concentrations by ~40 ppm (basalt) or ~140 ppm (harzburgite) by year 2100
110 in both the RCP4.5 and RCP8.5 climate change scenarios (Fig. 2a, b). Increasing the
111 application rate to 5 kg m^{-2} yr^{-1} over the same 20 Mkm^2 'hotspot' areas lowers the
112 atmospheric CO_2 concentration further by 150–180 ppm under both RCPs (Fig. 2c, d), with
113 an increasing effect at deeper soil mixing depths. For RCP4.5, atmospheric CO_2 by 2100 is
114 reduced from 540 ppm to 390–350 ppm (basalt) or 350–250ppm (harzburgite), sufficient to
115 play a major role in stabilizing climate and avoid seeding long-term amplifying climate
116 feedbacks[17] (Fig. 2). For the business-as-usual RCP8.5 scenario, however, the lowest
117 simulated CO_2 concentration by year 2100 in the high-end weathering scenario is still ~730
118 ppm (basalt) or 690–560 ppm (harzburgite) (Fig. 2d). This suggests even massive
119 intervention in Earth's carbon cycle with basalt is unable to drive atmospheric CO_2 down
120 close to the target of 350 ppm by 2100, an estimated requirement for restoring planetary
121 energy balance and stabilizing climate[17].

122 Future climate warming averted (WA) by engineering CO_2 removal through enhanced
123 weathering is dependent on climate sensitivity and the actual atmospheric CO_2 concentration.
124 Calculated end-of-century 'warming averted' figures for the enhanced weathering scenarios
125 using GENIE, which has a low-to-medium climate sensitivity, are summarized in Table 1.
126 For high application rates, WA ranges from 0.9–2.2°C for RCP4.5 and 0.7–1.6°C for RCP8.5
127 (Table 1). At low application rates, corresponding ranges of WA are 0.2–0.7°C for both
128 RCPs (Table 1). These numbers suggest that, theoretically at least, negative emissions from
129 enhanced weathering could play a role alongside conventional mitigation reducing net CO_2
130 emissions in limiting future warming[25].

Unmitigated future increases in atmospheric CO_2 will not only drive climate change but also ocean acidification, including reduced saturation of surface waters with respect to aragonite, threatening reef-building coral ecosystems[11-14]. Artificially enhanced tropical weathering increases land-to-ocean fluxes of alkalinity and dissolved inorganic carbon and raises freshwater pH to the upper range of tropical rivers (Supplementary Information). These fluxes, together with reduced atmospheric CO_2 (Fig. 2), tend to counter the negative impacts on ocean carbonate chemistry (Figs. 3 and 4). Our simulations driven by decreased CO_2 (Fig. 2) and increased alkalinity fluxes show that additions of 1 kg m^{-2} yr^{-1} of harzburgite or basalt across the weathering 'hotspots' can mitigate future ocean acidification by an average of around 0.1 pH units (Fig. 3a, b). A higher silicate application rate (5 kg m^{-2} yr^{-1}) reverses future surface ocean acidification under RCP4.5, restoring global mean surface ocean pH to year 2000 levels or even pre-industrial levels by 2100 (Fig. 3c). Even for RCP8.5, 5 kg m^{-2} yr^{-1} reduces ocean acidification by approximately two-thirds by year 2100 (Fig. 3d) (Supplementary Information).

Coral reef health is linked to the ocean's aragonite saturation state (Ω_a), which affects the rate at which corals can precipitate this crystalline mineral form of calcium carbonate and build skeletons[13,14]. Modern coral reefs generally occur where open ocean waters have a value of Ω_a above a postulated[14] critical threshold of ~3.5. But under RCP4.5, and especially RCP8.5, Ω_a at reef sites drops to <3.5 by 2100 (Fig. 4), potentially threatening them with extinction[14]. In simulations for RCP4.5 and RCP8.5, enhanced weathering with 1 kg m^{-2} yr^{-1} of silicates (basalt or harzburgite) and reduced atmospheric CO_2, generates conditions of Ω_a >3.5 across main regions of coral reef occurrence (Fig. 4a–e). Hence, although this low dosage is rather ineffective at reducing global CO_2 (Fig. 2), it has specific regional advantages in terms of helping protect coral reefs. Applications of either rock at high rates (5 kg m^{-2} yr^{-1}) markedly increase Ω_a above 3.5 in both RCP4.5 and RCP8.5 scenarios at low latitudes (Fig. 4c,f). Enhanced weathering on land could therefore be more effective at alleviating stressors on coral reef health, including ocean acidification, than enhanced open-ocean dissolution of olivine[26,27].

Our spatial and temporal analyses incorporate detailed plant-soil-climate interactions regulating soil mineral weathering rates. Driven by detailed geographical variations in projections of 21st century climate change and vegetation activity, they indicate the maximum potential of enhanced weathering for climate change mitigation, including amelioration of

ocean acidification. However, our scenarios represent a suite of idealized cases in which application of pulverised silicate rocks over forests is assumed to be achievable over large regions. Consequently, they help define the maximum potential CDR capacity of the approach. Not only will practical barriers to mineral transport and distribution on biodiverse tropical forests limit large-scale deployment, but roll-out on such a large-scale may be undesirable from both conservation and ecosystem services viewpoints. Deployment might be achievable in areas undergoing reforestation/afforestation or on agricultural lands where existing infrastructure could be utilized for rock grain distribution and management. However, well-documented field studies on graded spatial scales are needed prior to any significant implementation.

Large-scale geoengineering is ethically fraught[15] and poses dangers of both foreseeable and unforeseen consequences. Enhanced weathering employs naturally occurring minerals and reactions and therefore falls in the category of "soft geoengineering" along with reforestation, and agricultural techniques increasing soil carbon storage[28]. Nevertheless, it still requires comprehensive environmental impact assessments and dust mitigation strategies at production and deployment sites. Additionally, the production and distribution of pulverised rock carries health risks to anyone coming in contact with it because the particle sizes involved are respirable (Supplementary Information). Harzburgite, for example, includes asbestos-related minerals that carry health risks to local populations near application sites. However, carefully implemented, enhanced weathering may have added benefits, including fertilizing ocean and terrestrial CO_2 capture by marine diatoms[3,26,29] and tropical forests, respectively. Such effects, which are not considered here, could help offset energy costs[3,5] associated with extensive rock mining, grinding and transportation operations that might lower its sequestration capacity by ~8–33%.

Estimated implementation costs (combined capital and operational) for achieving an initial 50 ppm drawdown of atmospheric CO_2 are $60–600 trillion for mining, grinding and transportation, assuming no technological innovation, with similar associated additional costs for distribution (Supplementary Information). On this basis, costs of enhanced weathering as a 'negative emissions' option exceed an estimate of $50–200 trillion[17] for air capture of 50 ppm CO_2, but with the latter being less effective in reducing ocean acidification in important coral reef regions. These issues support calls for the alternative of a rising international carbon fee[17]. We proffer enhanced weathering not as a panacea for erasing impacts of fossil

fuel burning, but as a sobering indication of actions that may be required if fossil fuel emissions are not phased-down rapidly.

Methods

Methods and any associated references are available in the online version of the paper.

References

1 Seifritz, W. CO_2 disposal by means of silicates. *Nature* **345**, 486, doi:10.1038/345486b0 (1990).

2 Schuiling, R. D. & Krijgsman, P. Enhanced weathering: An effective and cheap tool to sequester CO_2. *Clim. Change* **74**, 349-354, doi:10.1007/s10584-005-3485-y (2006).

3 Köhler, P., Hartmann, J. & Wolf-Gladrow, D. A. Geoengineering potential of artificially enhanced silicate weathering of olivine. *Proc. Natl. Acad. Sci. U.S.A.* **107**, 20228-20233, doi:10.1073/pnas.1000545107 (2010).

4 Hartmann, J. *et al.* Enhanced chemical weathering as a geoengineering strategy to reduce atmospheric carbon dioxide, supply nutrients, and mitigate ocean acidification. *Rev. Geophys.* **51**, 113-149, doi:10.1002/rog.20004 (2013).

5 Moosdorf, N., Renforth, P. & Hartmann, J. Carbon dioxide efficiency of terrestrial enhanced weathering. *Environ. Sci. Technol.* **48**, 4809-4816, doi:10.1021/es4052022 (2014).

6 Taylor, L. L., Banwart, S. A., Leake, J. R. & Beerling, D. J. Modeling the evolutionary rise of ectomycorrhiza on sub-surface weathering environments and the geochemical carbon cycle. *Am. J. Sci.* **311**, 369-403, doi:10.2475/05.2011.01 (2011).

7 Taylor, L. L., Banwart, S. A., Valdes, P. J., Leake, J. R. & Beerling, D. J. Evaluating the effects of terrestrial ecosystems, climate and carbon dioxide on weathering over geological time: a global-scale process-based approach. *Philos. Trans. R. Soc. B-Biol. Sci.* **367**, 565-582, doi:10.1098/rstb.2011.0251 (2012).

8 Cao, L. *et al.* The role of ocean transport in the uptake of anthropogenic CO_2. *Biogeosciences* **6**, 375-390, doi:10.5194/bg-6-375-2009 (2009).

9 Hempel, S., Frieler, K., Warszawski, L., Schewe, J. & Piontek, F. A trend-preserving bias correction - the ISI-MIP approach. *Earth Syst. Dynam.* **4**, 219-236, doi:10.5194/esd-4-219-2013 (2013).

10 Taylor, K. E., Stouffer, R. J. & Meehl, G. A. An overview of CMIP5 and the experiment design. *Bull. Am. Met. Soc.* **93**, 485-498, doi:10.1175/BAMS-D-11-00094.1 (2011).

11 Caldeira, K. & Wickett, M. E. Anthropogenic carbon and ocean pH. *Nature* **425**, 365-365, doi:10.1038/425365a (2003).

12 Ciais, P. *et al.* in *Climate change 2013: The Physical Science Basis. Contribution of Working Group I to the Fifth Assessment Report of the Intergovernmental Panel on*

Climate Change (eds T. F. Stocker *et al.*) Ch. 6, 465-570 (Cambridge University Press, Cambridge, UK and New York, USA, 2013).

13 Turley, C. *et al.* The societal challenge of ocean acidification. *Marine Pollution Bull.* **60**, 787-792, doi:10.1016/j.marpolbul.2010.05.006 (2010).

14 Ricke, K. L., Orr, J. C., Schneider, K. & Caldeira, K. Risks to coral reefs from ocean carbonate chemistry changes in recent earth system model projections. *Environ. Res. Lett.* **8**, 6, doi:10.1088/1748-9326/8/3/034003 (2013).

15 Caldeira, K., Bala, G. & Cao, L. The science of geoengineering. *Annu. Rev. Earth Planet. Sci.* **41**, 231-256, doi:10.1146/annurev-earth-042711-105548 (2013).

16 United Nations Framework Convention on Climate Change, available at http://www.unfccc.int. (1992).

17 Hansen, J. *et al.* Assessing "dangerous climate change": required reduction of carbon emissions to protect young people, future generations and nature. *PLoS ONE* **8**, e81648, doi:10.1371/journal.pone.0081648 (2013).

18 Committee on Geoengineering Climate: Technical Evaluation and Discussion of Impacts; Board on Atmospheric Sciences and Climate; Ocean Studies Board; Division on Earth and Life Studies; National Research Council, Climate Intervention: Carbon Dioxide Removal and Reliable Sequestration, ISBN 978-0-309-30529-7. (National Academy of Sciences, Washington D. C., 2015).

19 Hartmann, J., Jansen, N., Dürr, H. H., Kempe, S. & Köhler, P. Global CO_2-consumption by chemical weathering: What is the contribution of highly active weathering regions? *Global Planet. Change* **69**, 185-194, doi:10.1016/j.gloplacha.2009.07.007 (2009).

20 Wignall, P. B. Large igneous provinces and mass extinctions. *Earth-Sci. Rev.* **53**, 1-33, doi:10.1016/s0012-8252(00)00037-4 (2001).

21 Hilf, H. H. The manuring of poor soils with basalt grit. *Forstarchiv.* **14**, 93-101 (1938).

22 de Villiers, O. D. Soil rejuvenation with crushed basalt in Mauritius Part I: Consistent results of world-wide interests. *Int. Sugar J.* **63**, 363-364 (1961).

23 Anda, M., Shamshuddin, J. & Fauziah, C. I. Increasing negative charge and nutrient contents of a highly weathered soil using basalt and rice husk to promote cocoa growth under field conditions. *Soil Tillage Res.* **132**, 1-11, doi:10.1016/j.still.2013.04.005 (2013).

24 Gillman, G. P., Burkett, D. C. & Coventry, R. J. Amending highly weathered soils with finely ground basalt rock. *Appl. Geochem.* **17**, 987-1001, doi:10.1016/S0883-2927(02)00078-1 (2002).

25 Gasser, T., Guivarch, C., Tachiiri, K., Jones, C. D. & Ciais, P. Negative emissions physically needed to keep global warming below 2 °C. *Nat Commun* **6**, doi:10.1038/ncomms8958 (2015).

26 Köhler, P., Abrams, J. F., Völker, C., Hauck, J. & Wolf-Gladrow, D. A. Geoengineering impact of open ocean dissolution of olivine on atmospheric CO_2, surface ocean pH and marine biology. *Environ. Res. Lett.* **8**, 014009 (2013).

27 Hangx, S. J. T. & Spiers, C. J. Coastal spreading of olivine to control atmospheric CO_2 concentrations: A critical analysis of viability. *Int. J. Greenhouse Gas Control* **3**, 757-767, doi:10.1016/j.ijggc.2009.07.001 (2009).

28 Royal Society Report - Geoengineering the climate: science, governance and uncertainty. Report No. RS1636, (The Royal Society, London, 2009).

29 Bernard, C. Y., Dürr, H. H., Heinze, C., Segschneider, J. & Maier-Reimer, E. Contribution of riverine nutrients to the silicon biogeochemistry of the global ocean – a model study. *Biogeosciences* **8**, 551-564, doi:10.5194/bg-8-551-2011 (2011).

Supplementary Information is linked to the online version of the paper at www.nature.com/nature

Acknowledgements We thank Yves Goddéris and Phil Renforth for helpful comments on the manuscript, Tim Elliot for earlier discussions, and gratefully acknowledge funding through an ERC Advanced grant to D.J.B. (CDREG, 32998). We acknowledge the World Climate Research Programme's Working Group on Coupled Modelling, which is responsible for CMIP, and we thank the climate modelling groups (Table S1) for producing and making available their model output. For CMIP the U.S. Department of Energy's Program for Climate Model Diagnosis and Intercomparison provides coordinating support and led development of software infrastructure in partnership with the Global Organization for Earth System Science Portals.

Author Contributions D.J.B. conceived the study with input from all co-authors. L.L.T. undertook weathering model development and simulations, J.Q. and R.M.S.T. undertook data analyses, P.A.K. and A.R. provided model set-up support and advice, M.R.L. analysed the CMIP5 climates. D.J.B. led the writing with contributions from all co-authors, especially J.H., A.R., J.Q. and L.L.T.

Author Information Reprints and permissions information is available at www.nature.com/reprints. The authors declare no competing financial interests. Correspondence and requests for materials should be addressed to D.J.B. (d.j.beerling@sheffield.ac.uk).

296 **Figure Legends**

297 **Figure 1. Enhanced weathering from pulverised silicate rock additions to the tropics**
298 **increases CO_2 consumption.** End-of-century CO_2 consumption by enhanced terrestrial
299 weathering with (**a**) dunite, (**b**) harzburgite or (**c**) basalt as a function of total rock applied,
300 defined as the product of rate and an increasing treated land area in the tropics (30°S to 30°N).
301 Simulations are shown for the Representative Concentration Pathway (RCP) 8.5; median and
302 range for five climate model simulations for each application scenario. Symbols indicate
303 reductions in CO_2 consumption and total rock applied when application is limited to 20 Mkm^2
304 of tropical weathering hotspots; symbol shape and fill denotes application rate and mixing
305 depth scenario, respectively, for each curve. Vertical red lines show estimated total resources
306 for each rock type (for basalt, solid, dashed and dot-dashed lines represent basalt resources in
307 each of the Ethiopian, Deccan and Paraná Traps, respectively). The shaded area denotes
308 uncertainty in upper values of global dunite resource availability (Supplementary
309 Information). Panels (**d**) to (**f**) display the corresponding ensemble ranges for high and low
310 application scenarios for each of five climate model simulations for both RCP8.5 and RCP4.5,
311 assuming a mixing depth of 30 cm.

312 **Figure 2. Enhanced weathering lowers atmospheric CO_2 with projected 21st century**
313 **climate change.** Effects of low additions (1 kg m^{-2} yr^{-1}) of silicate rock to 20 Mkm^2 of
314 tropical weathering hotspots for two mixing depths (10 cm and 30 cm) on the atmospheric
315 CO_2 concentration for (**a**) RCP4.5 (medium-level mitigation) and (**b**) RCP8.5 (business-as-
316 usual). Panels (**c**) and (**d**) show comparable results for the effect of higher additions (5 kg m^{-2}
317 yr^{-1}) of silicate rocks to the same areas of the tropics. In all panels, the pale blue line indicates
318 the 'control' run with RCP-driven weathering, without additions of silicate rock. Envelopes
319 and lines (solid 10 cm/dashed 30 cm) show the smoothed (five-year boxcar) ranges and
320 medians, respectively, of results from five climate models for each RCP.

Figure 3. Enhanced weathering ameliorates future ocean acidification caused by projected 21st century increases in atmospheric CO_2. Effects of increased alkalinity fluxes resulting from additions of 1 kg m^{-2} yr^{-1} of silicate rock to 20 Mkm^2 of tropical weathering hotspots mixed to two soil depths on global surface ocean pH for (**a**) RCP4.5 (medium-level mitigation) and (**b**) RCP8.5 (business-as-usual). Panels (**c**) and (**d**) show comparable results for the effect of higher additions (5 kg m^{-2} yr^{-1}) of silicate rocks to the tropics on global surface ocean pH for RCP4.5 and RCP8.5 respectively. Envelopes and lines (solid 10 cm/dotted 30 cm mixing depths) show the smoothed (five-year boxcar) ranges and medians, respectively, of results from five climate models for each RCP.

Figure 4. Enhanced weathering raises the aragonite saturation state of the ocean by 2100. Simulated global distribution of the aragonite saturation state (Ω_a) of the surface ocean in 2100 for RCP4.5 (**a**) no addition of silicate rocks, 1 kg m^{-2} yr^{-1} of (**b**) basalt and (**c**) harzburgite distributed over the tropics. Corresponding simulations for RCP8.5 are given in (**d**), (**e**) and (**f**) for applications of 5 kg m^{-2} yr^{-1}. Each panel displays in black the distribution of reef-building corals (www.reefbase.org). All simulations are for a mixing depth of 30 cm.

Methods

Terrestrial rock weathering modelling. Terrestrial vegetation delivers the carbon-energy flux in the form of photosynthate to roots and associated mycorrhizal fungal networks which fuels biotic rates of mineral dissolution[30]. In our rock weathering model, the sub-surface organic carbon flux is stoichiometrically coupled to the rate of primary production and the uptake of inorganic nutrient ions by roots and mycorrhizal fungi which regulate the ionic composition and charge balance of the microscopic region of soil pore fluids at the organism-mineral interface (the mycorrhizosphere)[6,7]. This balance controls local pore fluid pH and organic ligand concentrations at the reacting mineral surfaces that control the rates of mineral dissolution through well-described reaction mechanisms[31]. We therefore couple an extended version of a previously published rock weathering model[6,7] with the Sheffield Dynamic Global Vegetation Model (SDGVM)[32]. Our simulations employed fixed land use patterns[33]. The SDGVM simulates terrestrial carbon, nitrogen and water cycling by vegetation and soils including land surface net primary productivity (NPP), hydrology, autotrophic and heterotrophic soil respiration, and dissolved organic carbon pools[32]. SDGVM is comparable in its sensitivity of response to CO_2 and climate to other DGVMs[34,35].

In the extended weathering model, rainwater with an initial pH determined by the partial pressure and solubility of atmospheric $CO_{2(g)}$ and ion charge balance percolates through the soil at a rate determined by the SDGVM runoff. Soil solution chemistry is calculated both within and outside the mycorrhizosphere within the soil profile, which is divided into 10 layers specified at increasing depths, with runoff composition from each layer mixed and advected into the next layer. Mixing of bulk soil and mycorrhizosphere water is conceptualised as, but not explicitly parameterised as, hydrodynamic dispersion and diffusive exchange of bulk soil fluid solutes with the decreasing mycorrhizosphere volume with depth[6], and pore fluid transport to plant roots for transpiration. The model recalculates the soil solution chemistry of each layer, with the dissolution reaction progress of primary silicate minerals ceasing upon reaching the theoretical saturation state of the fluid with respect to the dissolving mineral. Thermodynamic equilibria constrain both the forward reaction for mineral dissolution (see Eq. 1 below) and the concurrent precipitation of secondary phases including kaolinite, gibbsite and amorphous silica which act as sinks for dissolved Al and Si released by weathering. On carbonate-bearing lithologies, pore fluids are equilibrated with any calcite, dolomite or gypsum which might be present before weathering of any silicate

minerals present takes place. This treatment assumes sufficient carbonates to maintain solubility equilibrium during the simulation time horizon and is not suitable for trace amounts of carbonate minerals which would become completely depleted in non-carbonate lithologies. Soil solution chemistry, therefore, depends on solubility equilibrium with existing carbonate or sulphate minerals, precipitation of secondary phases, including kaolinite and amorphous silica, and weathering of primary silicate minerals.

Underlying the weathering model is a rasterised version of the Hartmann & Moosdorf[36] lithological map for which we prepared a lithological database giving the proportions of the parent minerals in each rock type. Each rock type has its own mineral assemblage (see below), and each mineral *m* weathers according to the general rate law[37] with mineral-specific parameter values for *SA*, *k*, *n* and *E*:

$$Rate_m = SA_m \sum_i \left[k_{i,m}^{298.15} exp\left[\frac{-E_{i,m}}{R} \left(\frac{1}{T} - \frac{1}{298.15} \right) \right] a_i^{n_{i,m}} \left(1 - \left[\frac{Q_m}{Ksp_m} \right] \right) \right] \quad \text{Eq. (1)}$$

where $Rate_m$ is given in mol m^{-2} mineral s^{-1}, *SA* is mineral surface area (m^2), *i* is the individual weathering agent, such as $[H^+]$, $k_{i,m}$ is the rate constant, $E_{i,m}$ is the apparent activation energy (kJ mol^{-1}), *R* is the gas constant (kJ mol^{-1} K^{-1}), *T* is temperature (K), a_i is the molar activity of weathering agent *i* (mol l^{-1}) and $n_{i,m}$ is the reaction order. $Q_m = \prod_j a_j^{s_j}$ is the ion activity product of the soil solution, where a_j is the activity of solute *j* raised to the power of its stoichiometry s_j on the product side of the chemical equation describing the dissolution of mineral *m* (Tables S2, S3). Ksp_m is the solubility constant for mineral *m* (Table S2). Activities are approximated by concentrations.

The model accounts for changes in mineral surface area due to relief (standard deviation of orography) as described previously[7] and includes an empirical surface area correction for each rock type which accounts for age effects[38], internal porosity, grain size errors and deviation of particle shape from perfect spheres. Soil water residence times and riverine fluxes depend on run-off calculated by SDGVM. The model calculates monthly fluxes of CO_2 consumption, alkalinity (Ca^{2+}, Mg^{2+}, K^+ and Na^+) and dissolved inorganic carbon and is verified against water chemistry and discharge data from a global suite of river catchments

Validation. Simulated terrestrial fluxes of CO_2 consumed by rock weathering in 42 watersheds worldwide[39] using the CRU-3 climate[40] at 1° × 1° resolution are validated against fluxes derived from catchment-scale estimates based on stream-water chemistry

(Supplementary Information). We generated fluxes for basins in the World Resources Institute's shapefile[41] and compared these to the 45 basins (Table 3 in Ref. 39) where the basin names could be matched. Given the test aims to compare model and observed weathering rates, three catchments were rejected on the basis of markedly different basin areas or runoff (defined as two standard deviations of the mean residual). Therefore, 42 basins were retained for validation, except in the case of carbonate CO_2 consumption, where an additional five basins were excluded due to lack of carbonates in the modelled lithologies.

The response of modelled weathering rates in Iceland to temperature change accords with observed chemical weathering flux responses to climate warming over the past four decades in un-glaciated Icelandic catchments[42]. Regional responses also support the CO_2 and climate change sensitivity of our approach. Adopting a more complex soil weathering module coupled to a DGVM[43], another group predicted a similar increase in CO_2 consumption in the Mackenzie River arctic watershed from 355 ppm CO_2 and modern climate to 560 ppm CO_2 with an associated warmer climate, based on results from the RCP4.5 simulations (Supplementary Information). Estimated pH values of river run-off calculated from alkalinity fluxes and equilibrated to ambient CO_2, are comparable to measurements reported for a range of tropical river catchments (Supplementary Information).

Geoengineering simulations. For the atmospheric CO_2 concentration trajectories defined by the two RCPs considered here (RCP4.5 and RCP8.5), the five General Circulation Models (GCMs) produce monthly temperature, relative humidity and precipitation to drive SDGVM. Monthly climate datapoints closest to the desired coordinates are bilinearly interpolated in space before daily values for the month are estimated using climate statistics. These estimated daily climates force SDGVM. Distributed silicate rock grains are treated as perfect monomineralogical spheres with a nominal starting diameter of 10 μm. Initial total surface areas for the added silicates are calculated for each mineral using the total mass applied, specified diameter, weight fraction for the mineral, mineral specific gravity and the equations for the volume and surface area of a sphere. As weathering progresses, mass is removed and the fractional change in total surface area is estimated using the fractional change in mass raised to the power ⅔. This treatment assumes that each particle is a shrinking sphere. The total mass and surface area for each mineral are increased according to dose rate. No attempt is made to model a particle size distribution for either the starting silicate rock grain size or the individual mineral residues following weathering. Pulverized silicates are mixed with a

specified depth of soil, without modelling bioturbation processes or the transport behaviour of suspended materials in infiltrating water. Soil water residence times and riverine fluxes depend on runoff modelled by SDGVM. Mean reactive surface areas of autochthonous primary soil minerals are corrected for erosion and relief[7]. The model assumes no change in porosity or water movement with depth, and there is no preferential transport of different particle sizes.

Mineralogy of pulverized silicates. The mineralogy of each simulated pulverized silicate rock is listed in Table S4. The model basalt silicate mineralogy is based on the normative composition for a normal alkali tholeiitic basalt[44], neglecting some minor phases such as magnetite. Our dunite composition follows Kogel *et al.*[45]. We use the mineralogy of the Troodos harzburgite, with lizardite rather than chrysotile (asbestos) as this is the dominant serpentine near Troodos[46] and as it is sensible to avoid rocks with a large proportion of asbestos for health reasons. Our results are therefore conservative with respect to the proportion of unserpentinised olivine and the relative amounts of lizardite and chrysotile present.

GENIE Earth system global CO_2 and ocean biogeochemistry modelling. The climate and ocean circulation of the GENIE Earth system model has been calibrated by 2-D reanalysis fields of surface air temperature and humidity and 3-D observational fields of ocean distributions of temperature and salinity[47]. The carbon cycle is calibrated against observed ocean phosphate and alkalinity distributions[47,48]. The resulting marine carbon cycle has been extensively used and evaluated, including against observations of natural (e.g. $\Delta^{14}C$) and perturbed anthropogenic carbon cycling. GENIE is also compatible with observational uncertainty[8] and other (generally higher resolution) carbon cycle model responses to CO_2 perturbation[49-51]. The version used here is as summarized by Cao *et al.*[8] that includes a 76 m deep surface ocean and the cycling of Fe described by Annan and Hargreaves[52] (except with biological uptake following Doney *et al.*[53]), but lacks a mixed layer scheme. Our results therefore represent a pessimistic case for weathering and in the real world one might have a slightly shallower surface layer with even higher saturation. The addition of Fe co-limitation of marine biological export results in a <1% change in the projected year 1994 anthropogenic CO_2 inventory compared to the PO_4-only model[8].

We simulated the effects of CO_2 consumption by enhanced weathering on atmospheric CO_2 drawdown and ocean biogeochemistry in two steps. First, we diagnosed the annual CO_2

462 emissions compatible with a particular RCP CO_2 concentration projection over the 21st
463 century by prescribing that CO_2 curve and backing-out emissions. Cross-checking these
464 diagnoses by performing forward simulations with annual CO_2 emissions in the absence of
465 enhanced weathering reproduced the RCP4.5 and RCP8.5 CO_2 curves to within 1 ppm. Then,
466 for each application scenario, we subtracted the annual CO_2 consumption due to enhanced
467 weathering from the diagnosed RCP emissions and forced GENIE with the remainder.

468 The ocean biogeochemistry simulations incorporate reduced atmospheric CO_2 and
469 increases in the alkalinity and dissolved inorganic carbon fluxes. In each case, those for
470 2005–2015 and 2089–2099 are transferred to a 36 × 36 global grid, migrating land fluxes on
471 the weathering model continents to the ocean following standard directional paths. GENIE
472 linearly interpolated these flux forcings for intermediate years. All GENIE runs were based
473 on the same starting state, comprising a 10,000-year pre-industrial spin-up followed by a
474 transient experiment forced by historical changes in atmospheric CO_2 concentration up until
475 year 2006 as described in Cao *et al.*[8] and Ridgwell *et al.*[48].

476

477 30 Quirk, J., Andrews, M. Y., Leake, J. R., Banwart, S. A. & Beerling, D. J.
478 Ectomycorrhizal fungi and past high CO_2 atmospheres enhance mineral weathering
479 through increased below-ground carbon-energy fluxes. *Biol. Lett.* **10**,
480 doi:10.1098/rsbl.2014.0375 (2014).
481 31 Brantley, S. L. in *Kinetics of Water-Rock Interaction* (eds Susan L. Brantley, James D.
482 Kubicki, & F. Art White) Ch. 5, 151-210 (Springer, 2008).
483 32 Woodward, F. I. & Lomas, M. R. Vegetation dynamics - simulating responses to climatic
484 change. *Biol. Rev.* **79**, 643-670, doi:10.1017/s1464793103006419 (2004).
485 33 Bartholomé, E. & Belward, A. S. GLC2000: a new approach to global land cover
486 mapping from Earth observation data. *Int. J. Remote Sens.* **26**, 1959-1977,
487 doi:10.1080/01431160412331291297 (2005).
488 34 Friend, A. D. *et al.* Carbon residence time dominates uncertainty in terrestrial vegetation
489 responses to future climate and atmospheric CO_2. *Proc. Natl. Acad. Sci. U.S.A.* **111**,
490 3280-3285, doi:10.1073/pnas.1222477110 (2014).
491 35 Sitch, S. *et al.* Evaluation of the terrestrial carbon cycle, future plant geography and
492 climate-carbon cycle feedbacks using five Dynamic Global Vegetation Models

(DGVMs). *Glob. Change Biol.* **14**, 2015-2039, doi:10.1111/j.1365-2486.2008.01626.x (2008).

36 Hartmann, J. & Moosdorf, N. The new global lithological map database GLiM: A representation of rock properties at the Earth surface. *Geochem. Geophys. Geosys.* **13**, doi:10.1029/2012gc004370 (2012).

37 Palandri, J. L. & Kharaka, Y. K. A compilation of rate parameters of water-mineral interaction kinetics for application to geochemical modeling. Report No. 2004-1068, 1-64 (U.S. Geological Survey, Menlo Park, California, 2004).

38 White, A. F. & Brantley, S. L. The effect of time on the weathering of silicate minerals: why do weathering rates differ in the laboratory and field? *Chem. Geol.* **202**, 479-506, doi:10.1016/j.chemgeo.2003.03.001 (2003).

39 Gaillardet, J., Dupré, B., Louvat, P. & Allègre, C. J. Global silicate weathering and CO_2 consumption rates deduced from the chemistry of large rivers. *Chem. Geol.* **159**, 3-30, doi:10.1016/S0009-2541(99)00031-5 (1999).

40 Mitchell, T. D. & Jones, P. D. An improved method of constructing a database of monthly climate observations and associated high-resolution grids. *Int. J. Climatology* **25**, 693-712, doi:10.1002/joc.1181 (2005).

41 Food Agriculture Organization of the United Nations. FAO GEONETWORK. (FAO, Rome, Italy, 2014).

42 Gislason, S. R. *et al.* Direct evidence of the feedback between climate and weathering. *Earth. Planet. Sci. Lett.* **277**, 213-222, doi:10.1016/j.epsl.2008.10.018 (2009).

43 Beaulieu, E., Godderis, Y., Donnadieu, Y., Labat, D. & Roelandt, C. High sensitivity of the continental-weathering carbon dioxide sink to future climate change. *Nature Clim. Change* **2**, 346-349, doi:10.1038/nclimate1419 (2012).

44 Nockolds, S. R. Average chemcal compositions of some igneous rocks. *Geol. Soc. Am. Bull.* **65**, 1007-&, doi:10.1130/0016-7606(1954)65[1007:accosi]2.0.co;2 (1954).

45 Kogel, J. E., Trivedi, N. C., Barker, J. M. & Krukowski, S. T. *Industrial minerals and rocks - commodities, markets, and uses*. 7th edn, (Society for Mining, Metallurgy, and Exploration, 2006).

46 Magaritz, M. & Taylor, H. P. Oxygen and hydrogen isotope studies of serpentinization in Troodos ophiolite complex, Cyprus. *Earth. Planet. Sci. Lett.* **23**, 8-14, doi:10.1016/0012-821x(74)90023-5 (1974).

525 47 Price, A. R., Myerscough, R. J., Voutchkov, I. I., Marsh, R. & Cox, S. J. Multi-objective
526 optimization of GENIE Earth system models. *Philos. Trans. R. Soc. A-Math., Phys., &*
527 *Engineer. Sci.* **367**, 2623-2633, doi:10.1098/rsta.2009.0039 (2009).
528 48 Ridgwell, A. *et al.* Marine geochemical data assimilation in an efficient Earth System
529 Model of global biogeochemical cycling. *Biogeosciences* **4**, 87-104, doi:10.5194/bg-4-
530 87-2007 (2007).
531 49 Archer, D. *et al.* Atmospheric lifetime of fossil fuel carbon dioxide. *Annu. Rev. Earth*
532 *Planet. Sci.* **37**, 117-134, doi:10.1146/annurev.earth.031208.100206 (2009).
533 50 Eby, M. *et al.* Historical and idealized climate model experiments: an intercomparison of
534 Earth system models of intermediate complexity. *Clim. Past* **9**, 1111-1140,
535 doi:10.5194/cp-9-1111-2013 (2013).
536 51 Goodwin, P., Williams, R. G., Ridgwell, A. & Follows, M. J. Climate sensitivity to the
537 carbon cycle modulated by past and future changes in ocean chemistry. *Nature Geosci.* **2**,
538 145-150, doi:10.1038/ngeo416 (2009).
539 52 Annan, J. D. & Hargreaves, J. C. Efficient identification of ocean thermodynamics in a
540 physical/biogeochemical ocean model with an iterative Importance Sampling method.
541 *Ocean Model.* **32**, 205-215, doi:10.1016/j.ocemod.2010.02.003 (2010).
542 53 Doney, S. C., Lindsay, K., Fung, I. & John, J. Natural variability in a stable, 1000-yr
543 global coupled climate–carbon cycle simulation. *J. Clim.* **19**, 3033-3054,
544 doi:10.1175/JCLI3783.1 (2006).

545

Table 1. Projected mean global air temperature and change in temperature at year 2100. Values show mean ± S.D. of five climate models (CMIP5) for the change in end-of-century mean global temperature simulated with the GENIE Earth system model using revised CO_2 trajectories associated with each rock type and application rate with an applied rock mixing depth of 30 cm (Figure 2).

	Warming at 2100 (°C)		Warming averted at 2100 (°C)[a]	
	RCP 4.5	RCP 8.5	RCP 4.5	RCP 8.5
Control (no enhanced weathering)[b]	1.4 ± 0.01	3.0 ± 0.01	n/a	n/a
IPCC range of projected warming[c] [Ref.12]	1.1 – 2.6	2.6 – 4.8	n/a	n/a
Enhanced weathering scenario				
Harzburgite (1 kg m^{-2} yr^{-1})	0.8 ± 0.04	2.5 ± 0.04	0.7 ± 0.04	0.5 ± 0.04
Harzburgite (5 kg m^{-2} yr^{-1})	−0.77 ± 0.2	1.4 ± 0.1	2.2 ± 0.2	1.6 ± 0.1
Basalt (1 kg m^{-2} yr^{-1})	1.21 ± 0.02	2.8 ± 0.01	0.2 ± 0.02	0.2 ± 0.01
Basalt (5 kg m^{-2} yr^{-1})	0.5 ± 0.05	2.25 ± 0.05	0.9 ± 0.05	0.7 ± 0.05

[a]Relative to control (no enhanced weathering); [b]Relative to 2005; [c]Relative to 1986 – 2005

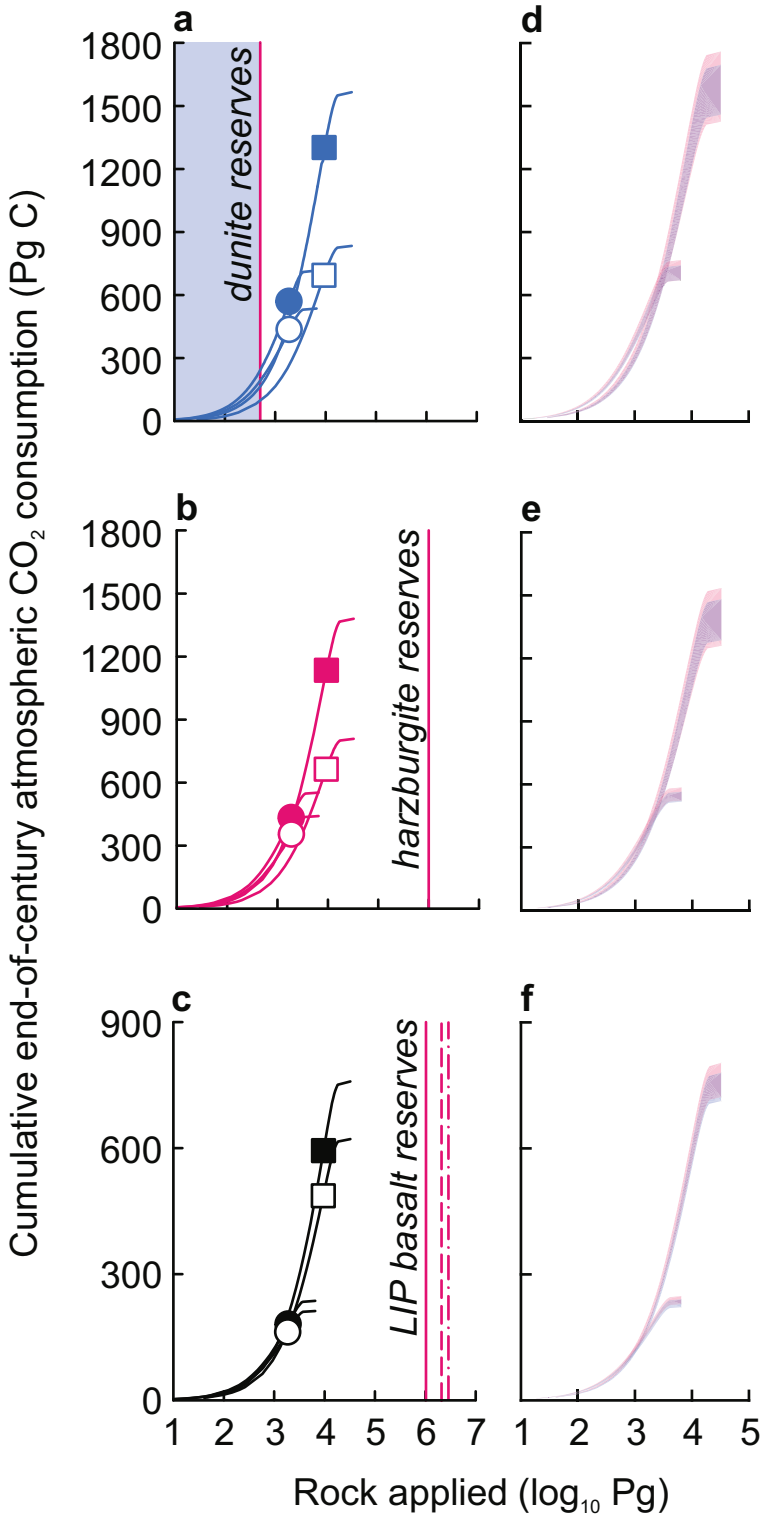
a
b
c
d
e
f
dunite reserves
harzburgite reserves
LIP basalt reserves
1800
1500
1200
900
600
300
0
1 2 3 4 5 6 7
1 2 3 4 5
Cumulative end-of-century atmospheric CO_2 consumption (Pg C)
Rock applied (log_{10} Pg)
Application rate:
squares 5 kg m^{-2} yr^{-1}
circles 1 kg m^{-2} yr^{-1}
Mixing depth:
filled 30 cm
open 10 cm
RCP:
4.5
8.5

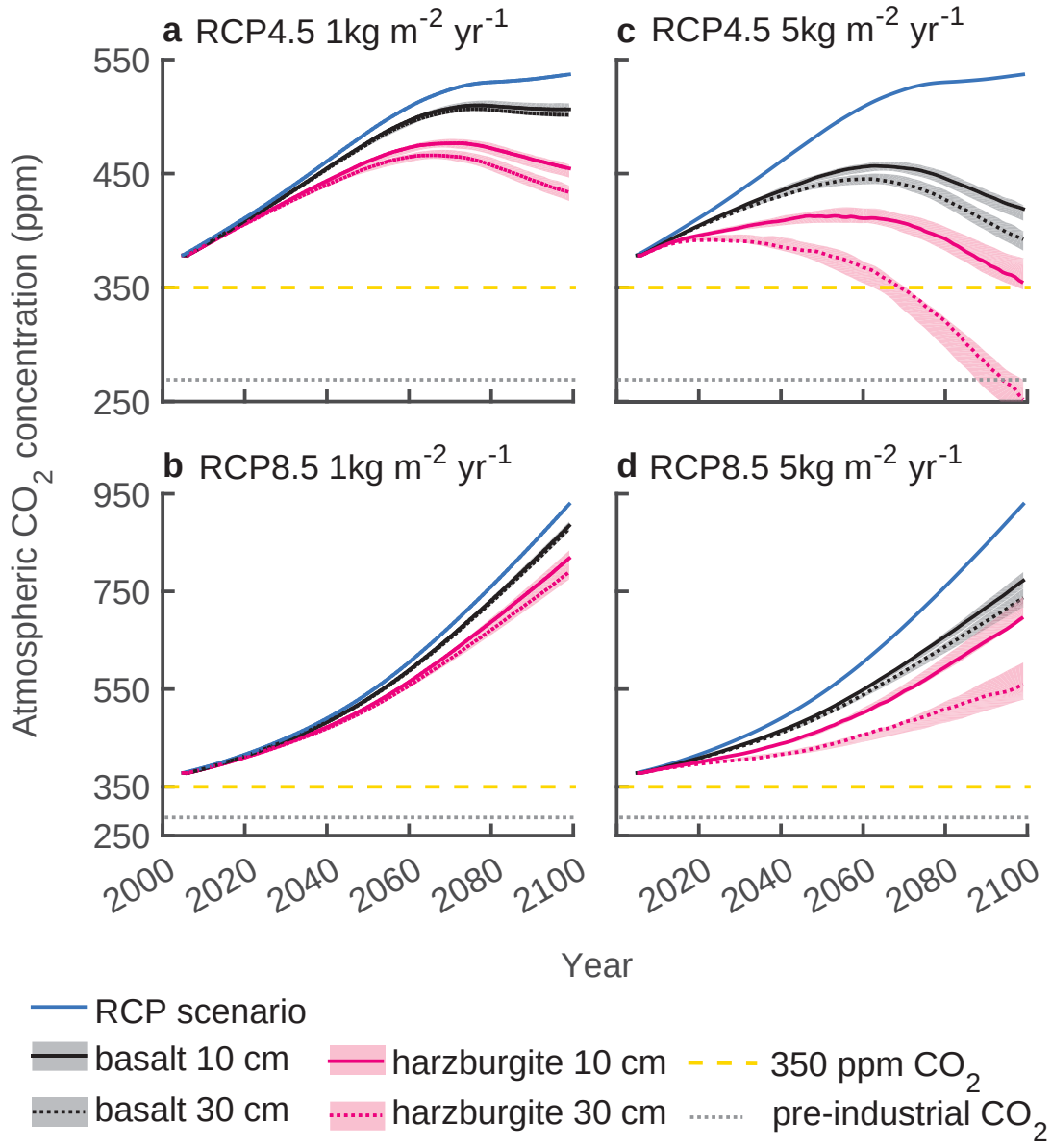
a RCP4.5 1kg m-2 yr-1
c RCP4.5 5kg m-2 yr-1
b RCP8.5 1kg m-2 yr-1
d RCP8.5 5kg m-2 yr-1
Atmospheric CO2 concentration (ppm)
550
450
350
250
950
750
550
350
250
2000
2020
2040
2060
2080
2100
Year
RCP scenario
basalt 10 cm
basalt 30 cm
harzburgite 10 cm
harzburgite 30 cm
350 ppm CO2
pre-industrial CO2

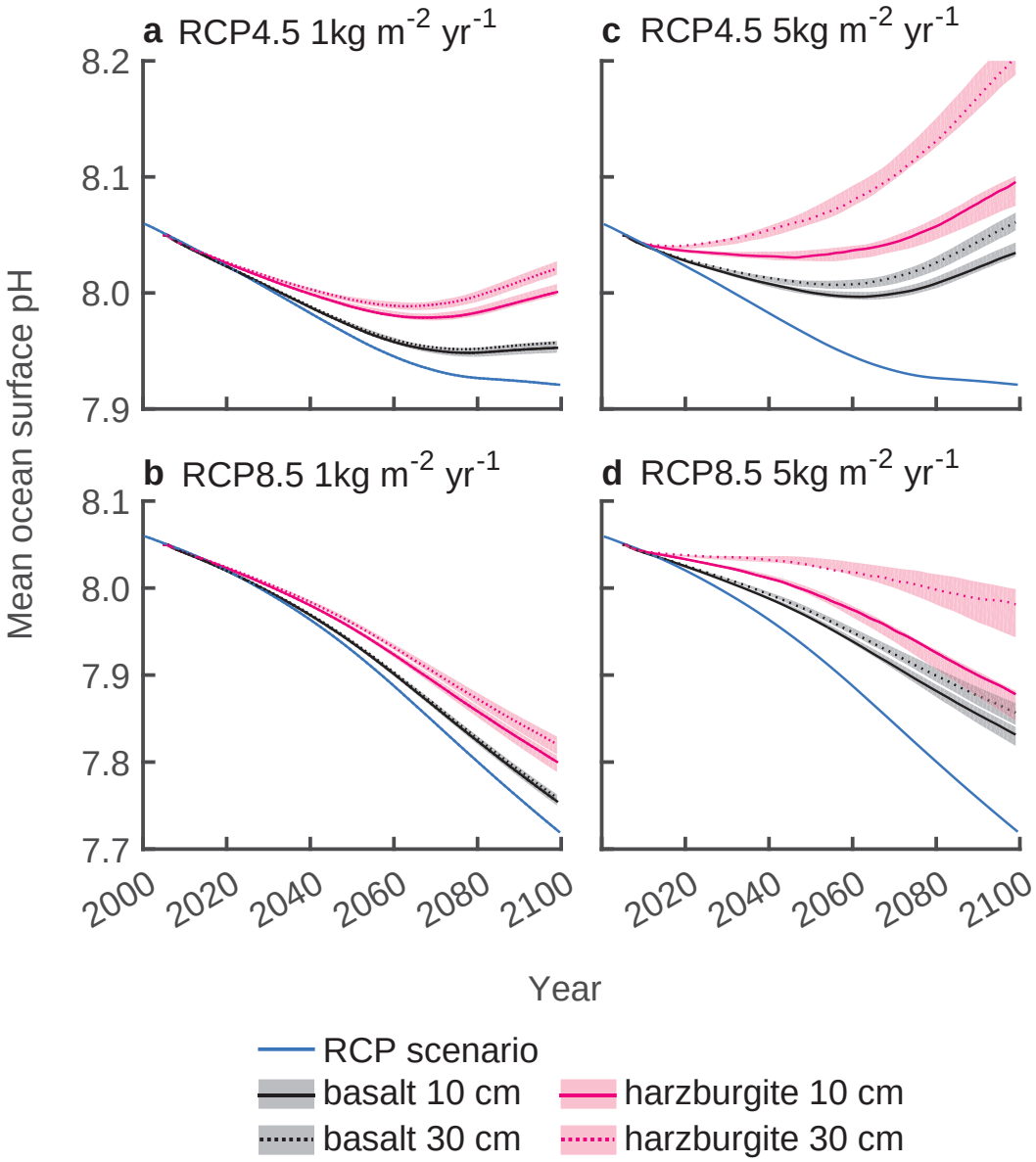
a RCP4.5 1kg m-2 yr-1
c RCP4.5 5kg m-2 yr-1
b RCP8.5 1kg m-2 yr-1
d RCP8.5 5kg m-2 yr-1
Mean ocean surface pH
8.2
8.1
8.0
7.9
8.1
8.0
7.9
7.8
7.7
2000
2020
2040
2060
2080
2100
Year
RCP scenario
basalt 10 cm
harzburgite 10 cm
basalt 30 cm
harzburgite 30 cm

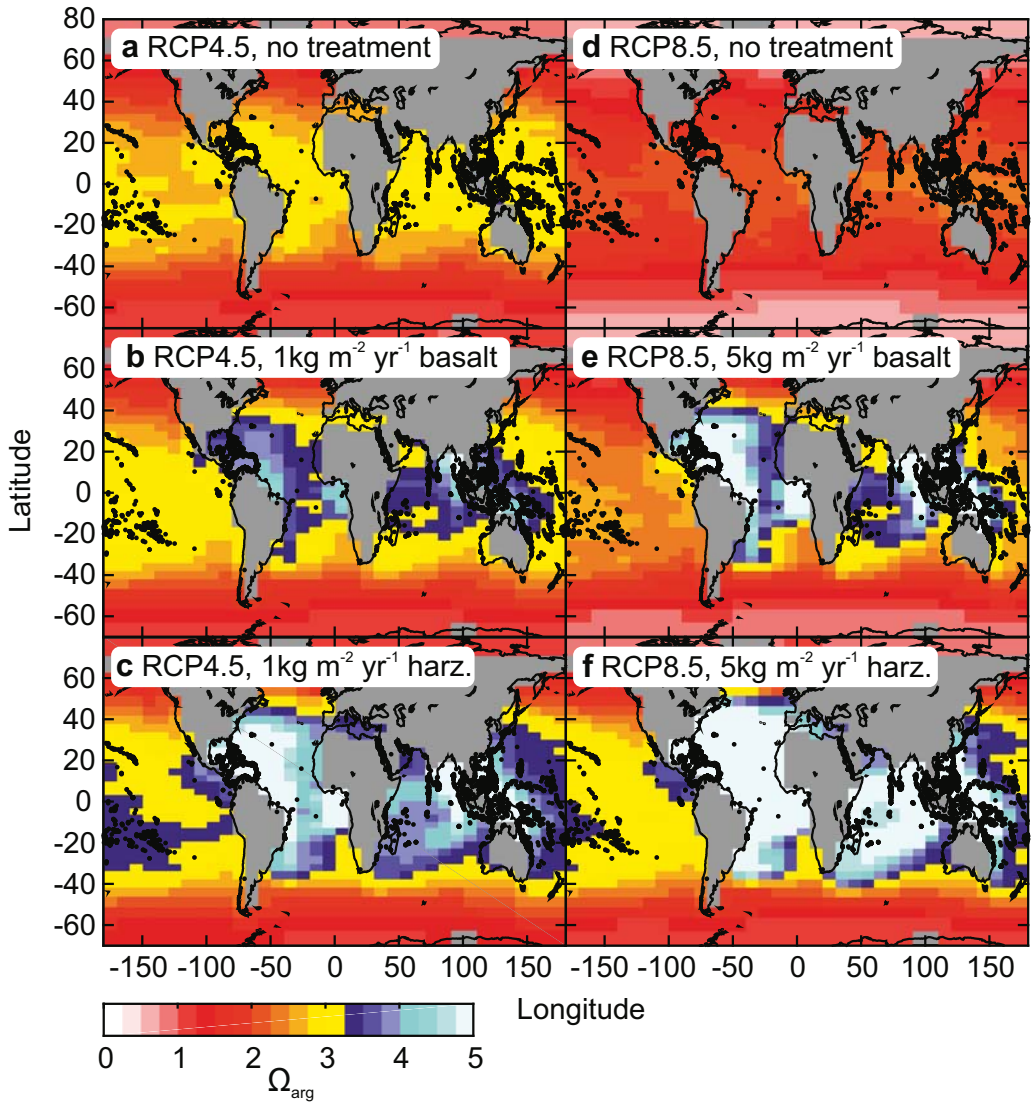
a RCP4.5, no treatment
d RCP8.5, no treatment
b RCP4.5, 1kg m-2 yr-1 basalt
e RCP8.5, 5kg m-2 yr-1 basalt
c RCP4.5, 1kg m-2 yr-1 harz.
f RCP8.5, 5kg m-2 yr-1 harz.
Latitude
80
60
40
20
0
-20
-40
-60
-150 -100 -50 0 50 100 150
Longitude
0 1 2 3 4 5
Ωarg